iScience

CellPress
OPEN ACCESS

Article

Dynamic segregation and integration of brain functional networks associated with emotional arousal

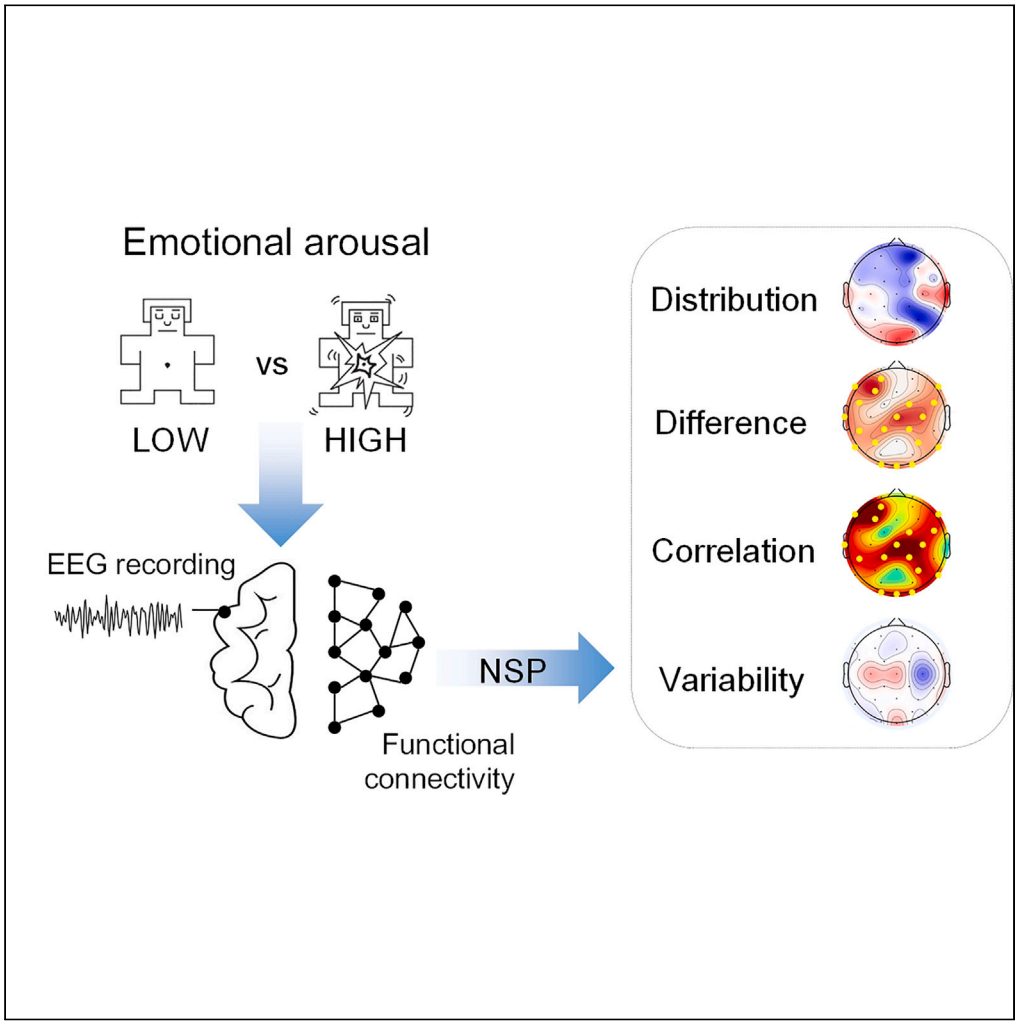

Lv Zhou, Yong Xie, Rong Wang, Yongchen Fan, Ying Wu

wying36@mail.xjtu.edu.cn

Highlights

Dynamic brain states were evaluated by the nested-spectral partition approach

Emotion-related network integration was enhanced in frontal and right parietal regions

Dwell time of regional integration was mostly related to the arousal ratings

Zhou et al., iScience 26, 106609
May 19, 2023
https://doi.org/10.1016/j.isci.2023.106609

iScience

CellPress
OPEN ACCESS

Article

Dynamic segregation and integration of brain functional networks associated with emotional arousal

Lv Zhou,[1,2,3] Yong Xie,[1,2] Rong Wang,[1,4] Yongchen Fan,[1,2] and Ying Wu[1,2,3,5,*]

SUMMARY

The organization of brain functional networks dynamically changes with emotional stimuli, but its relationship to emotional behaviors is still unclear. In the DEAP dataset, we used the nested-spectral partition approach to identify the hierarchical segregation and integration of functional networks and investigated the dynamic transitions between connectivity states under different arousal conditions. The frontal and right posterior parietal regions were dominant for network integration whereas the bilateral temporal, left posterior parietal, and occipital regions were responsible for segregation and functional flexibility. High emotional arousal behavior was associated with stronger network integration and more stable state transitions. Crucially, the connectivity states of frontal, central, and right parietal regions were closely related to arousal ratings in individuals. Besides, we predicted the individual emotional performance based on functional connectivity activities. Our results demonstrate that brain connectivity states are closely associated with emotional behaviors and could be reliable and robust indicators for emotional arousal.

INTRODUCTION

Emotion is a complicated blend of multiple affects and involves both situation perception and cognitive processing,[1–3] which is often quantified based on arousal, valence, and dominance dimensions.[4,5] Among these scales, arousal reflects the degree of behavioral awareness, increasing from inactive emotional states (sleepy, calm, depressed) to intensive states (excited, afraid, delighted).[5,6] High emotional arousal conditions are related to enhanced cognitive performance such as attention[7] and working memory,[8–10] whereas extreme emotional arousal (hyper-arousal or hypo-arousal) is associated with affective disorders such as anxiety and depression.[11,12] Therefore, investigating the neurophysiological mechanism of emotions with diverse arousal levels is important for affective computing as well as emotion-related illness.

Emotion often refers to neural activations in multiple brain regions involving the frontal, temporal, occipital, and parietal regions,[13–16] but focusing on regional activities is insufficient to reveal the neural mechanism of emotion.[17] It has attracted increasing attention that complex human behaviors are underpinned by the functional cooperation between brain regions rather than by a single item.[18–23] Emotional behaviors were also found to be supported by the dynamic organization of brain sub-networks,[24] for example, high arousal was associated with increased brain activity across visual and dorsal attention networks.[25] Functional connectivity (FC), which measures the correlation or synchronization between regions, provides a powerful tool to study emotion mechanisms in large-scale network models and has been proven to be effective in emotion recognition.[17,26]

In brain functional networks, modularity is a typical feature wherein the connectivity of regions within modules is strong and the connectivity between modules is relatively weak.[27] This topological structure allows segregated and integrated neural information processing and is closely related to cognition and brain disorders.[28,29] For example, global integration, which is supported by long-range information communication among brain areas, is commonly enhanced during cognitive tasks with heavy mental load.[20,30,31] While during vigilance, motor learning and sustaining attention tasks, brain functional organization tends to be more segregated with stronger information processing within specific regions.[29] However, how brain network integration and segregation support different emotional arousal behaviors is still unclear.[17,32]

[1]School of Aerospace Engineering, Xi'an Jiaotong University, Xi'an 710049, China

[2]State Key Laboratory for Strength and Vibration of Mechanical Structures, Xi'an 710049, China

[3]National Demonstration Center for Experimental Mechanics Education, Xi'an Jiaotong University, Xi'an 710049, China

[4]College of Science, Xi'an University of Science and Technology, Xi'an 710054, China

[5]Lead contact

*Correspondence: wying36@mail.xjtu.edu.cn

https://doi.org/10.1016/j.isci.2023.106609

In addition to modular organization, the brain is a dynamic system that fluctuates over seconds or even milliseconds with the considerable dynamic reconfiguration of functional network.[30,33–36] The transitions between integrated and segregated states of large-scale brain functional networks support rapid behavioral adaptation.[30,37] Due to its high temporal resolution, EEG is powerful in the long-time prediction of intra-individual differences[38] and automatic seizure identification,[39] and is also an appropriate technique for assessing the transitions of brain connectivity states affected by cognitive activities. Previous EEG research focusing on eye conditions has found that brain connectivity states and their dynamic transitions are highly related to resting-state condition.[40] In working memory tasks, both segregation and integration alternately dominated the functional configurations.[41] In particular, Yuvaraj et al. used EEG-based functional connectivity analysis to reveal the changes in brain interactions related to emotional states and reported increased coherence when viewing positive emotion compared with negative emotion.[42] However, the association between the dynamic reconfiguration of brain functional networks and emotional behaviors has rarely been explored.

To address the above questions, we evaluated the dynamic functional connectivity (dFC) based on the DEAP EEG dataset during emotional stimulus using sliding time windows.[30,43] This dataset has been widely used to test the performance of emotion recognition,[16,17,44] but is rarely utilized to analyze the relationship between emotional ratings and brain network parameters. We quantified the integration, segregation, and their transitions by a nest-spectral partition (NSP) method. This method detects modules across multiple levels in brain functional networks[37,45] and has been found to be more powerful in linking brain networks to cognitive abilities and the clinical scores of brain disorders.[46] We first investigated the heterogeneous responses of regions to emotional stimuli in different frequency bands. Second, we partitioned the emotional stimulus into high and low arousal conditions and compared the difference in dynamic functional organizations between the two conditions. We then studied whether the dynamics of brain functional networks are associated with emotion arousal ratings. Finally, we investigated whether the brain measures based on the NSP method can explain the individual variability in response to emotional stimuli.

RESULTS

We used the public DEAP dataset from 32 participants. The EEG signals were recorded from 32 electrodes during 40 emotional stimuli and the continuous arousal levels of participants were also included.[4] *Phase locking value* (PLV)-based dFC networks (N = 32 channels) in four frequency bands (θ: 4–7; α: 8–13 Hz; β: 14–30 Hz; γ:30–45 Hz) were constructed through the sliding time window method (see STAR Methods). Using the NSP method, the time-averaged integration strength (M_{in}), segregation strength (M_{se}), dwell time of integration state (T_{in}), and switching frequency (f_{IS}) were calculated to analyze brain connectivity state transitions under different arousal levels (Figure 1). These measures were also obtained for regions.

Regional heterogeneous performance during emotional stimuli

We first investigated which regions have major contributions to network segregation and integration during emotional stimuli. In the theta band, the temporo-parietal, right posterior parietal, and frontal regions, except for FP1 and AF3, showed higher integration, indicating that these regions play an important role in integrating information across the large-scale network during emotional stimuli. For the alpha band, the frontal and right posterior parietal regions had stronger integration strength and weaker time-averaged segregation. In the beta and gamma bands, the distribution of high integration was located in the frontal regions (excluding the left prefrontal areas) and right posterior parietal regions. Conversely, the bilateral temporal and occipital regions showed higher segregation strength in the theta band, meaning that these regions are more responsible for local interaction. The bilateral temporal, left temporo-parietal and occipital regions had high segregation strength in the alpha band. This segregation was more pronounced at bilateral temporal regions in the beta band and at broader areas, including left frontal regions in the gamma band.

During the dynamic transitions of brain networks between segregation and integration states, all regions except for the left and right temporal, and occipital regions dwelled longer in the integration state in the theta band (Figure 2). In the alpha band, the dwell time at integration state was longer in the frontal and right posterior parietal regions and shorter in the temporal, left temporo-parietal and occipital regions. However, this long dwell time was diminished in frontal regions in the beta and gamma bands and was located in the midline and right posterior parietal regions. Switching frequency was larger in the left temporo-parietal, right temporal, and occipital regions in the alpha band, indicating a more frequent transition

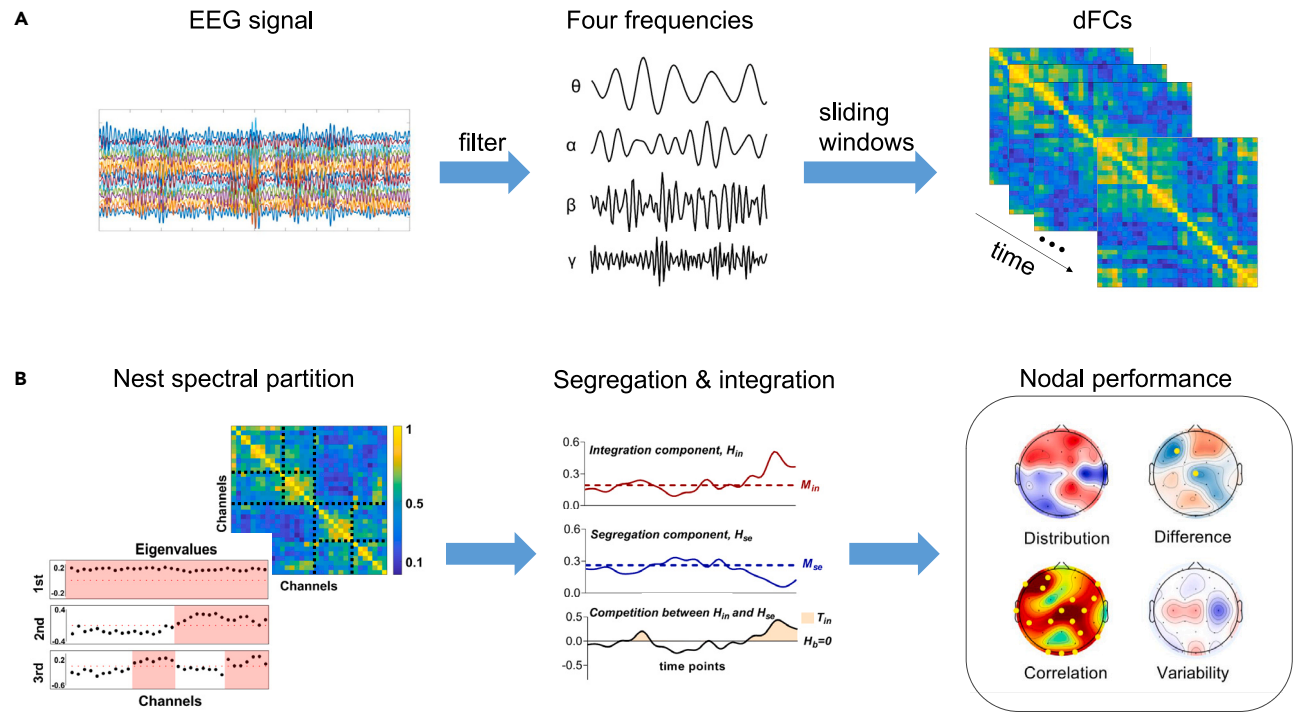

Figure 1. Analysis schematic illustration

EEG data were filtered into four frequency bands.

(A) The sliding window method was used to construct dFC by calculating the PLV between channels.

(B) For each FC network, the nested-spectral partition (NSP) method was applied to obtain the hierarchical modules that correspond to eigenvectors with different orders (here shown the first three levels), and the integration component H_{in}, segregation component H_{se} and their competition $H_B = H_{in}$-H_{se} were obtained. Based on the time series of dynamic H_{in}, H_{se}, and $H_{B,}$ we defined the dynamic brain network measures integration strength M_{in}, segregation strength M_{se}. Dwell time at integration state T_{in} and switch frequency between segregation and integration states f_{IS}. These measures were mapped to regions and thus the regional analysis can be performed.

between segregated and integrated states. Similar flexible transitions were also found in theta, beta, and gamma bands, but these three bands covered broader regions, including prefrontal electrodes.

Overall, during emotional stimuli, frontal and right posterior parietal regions had higher integration effects (M_{in}, T_{in}), whereas bilateral temporal, left temporo-parietal and occipital regions had stronger segregation, accompanied by frequent state transitions.

Higher network integration in the high emotional arousal condition

According to the arousal rating (1–9 scores), we partitioned 40 trials into low arousal (LA) condition trials (rating 1–4) and high arousal (HA) condition trials (rating 6–9) for each participant. We investigated the difference in functional organization between LA and HA conditions. In all frequency bands, brain networks had higher global integration strength M_{in} at HA relative to LA, but these differences were insignificant (Figure 3A). Although the segregation component M_{se} showed a nonsignificant difference between HA and LA in theta and alpha bands ($p = 0.591$ and 0.541, respectively), it was significantly smaller at HA than at LA in beta and gamma bands ($p = 0.026$ and 0.028, respectively), suggesting weaker global segregation for high emotional arousal levels in high-frequency bands.

At the local scale, regions had similar contribution patterns to segregation and integration at both HA and LA (see Figure S1). In the alpha band, left prefrontal regions had the highest increased integration component at HA relative to LA. In other frequency bands, similar differences in integration were also observed in the left frontal, central parietal, and left temporal regions, but the regional difference was weak in the theta band compared with the results of the beta and gamma bands. These alterations were insignificant after multiple comparison correction (all $p > 0.05$, FDR corrected). For the segregation strength, the left frontal and central parietal regions in the alpha band had the largest increase in LA, but the alterations were

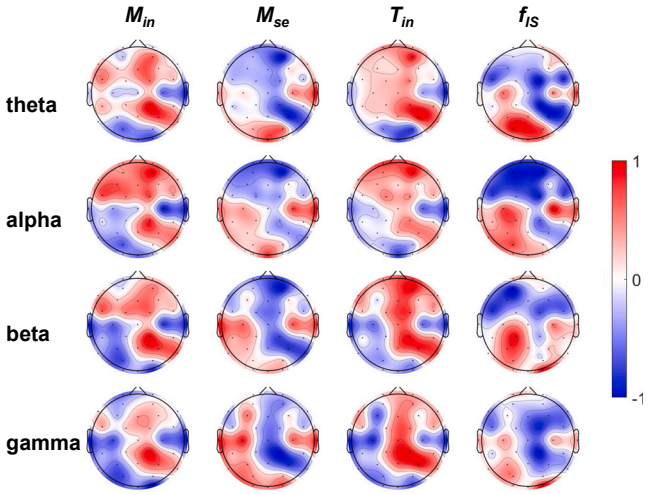

Figure 2. Normalized distributions of network measures on regions during emotional stimuli, averaged across all subjects and trials

insignificant (all $p > 0.05$, FDR corrected). In theta, beta, and gamma bands, the regions located near frontal (AF3, F3, F7, F8, F4), left temporal (T7), and parietal (FC2, Cz, CP1, FC6, C4, CP2, P4, CP5) had significantly increased M_{se} in HA relative to LA (all $p < 0.05$, FDR corrected). Besides, decreased segregation in theta band was also significant in occipital regions (O1, Oz). The above results reveal that HA corresponds to lower network segregation and is associated with broader regions mainly distributed in the frontal, left temporal, and parietal regions.

High arousal level recruits a more stable brain transition

We next studied the dynamic transition between segregated and integrated states at different arousal conditions. The brain at HA had significantly longer dwell time at the integrated states in theta, beta, and gamma bands ($p = 0.004$, 0.003, and 0.002, respectively), but an insignificant change in the alpha band ($p = 0.113$) (Figure 4A). At the local scale, all brain regions showed significantly increased dwell time at integration state in the theta band under HA condition, except for the central frontal, right temporal, and parieto-occipital regions. In the alpha band, the left frontal and central parietal regions under HA condition had significantly increased dwell time ($p < 0.05$, FDR corrected). In the beta and gamma bands, most regions had a significantly higher dwell time at HA than that at LA ($p < 0.05$, FDR corrected), among those brain regions, the left frontal and right occipital regions had the largest alteration.

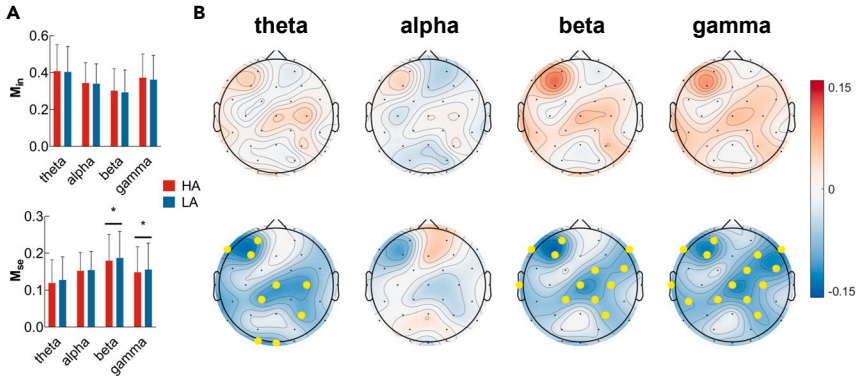

Figure 3. Time-averaged integration and segregation at different arousal states

(A) Integration strength M_{in} (upper) and segregation strength M_{se} (lower) under two arousal conditions. *$p < 0.05$.

(B) The difference in regional M_{in} (upper) and M_{se} (lower) between HA and LA conditions in four frequency bands. The regions with significant alterations were highlighted with yellow points ($p < 0.05$, FDR corrected).

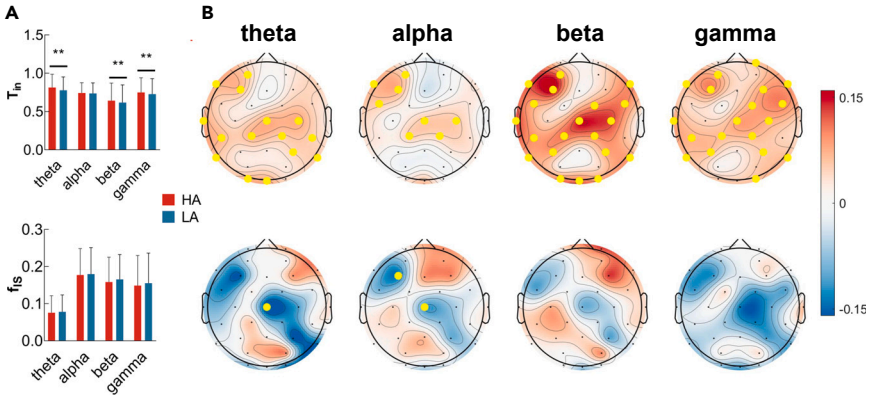

Figure 4. Dynamic analysis of the brain under HA and LA conditions

(A) Dwell time at integration states (upper) and switching frequency (lower). **p < 0.01.

(B) Regional differences in dwell time and switching frequency between the HA and LA conditions. The electrodes with significant changes are highlighted with yellow points (p < 0.05, FDR corrected).

In addition, when the brain was under HA condition, it was transitioning between segregation and integration states less frequently than that at LA, but the difference was insignificant for all bands (Figure 4A). However, in the alpha band, the frontal (F3, p = 0.033, FDR corrected) and central areas (Cz, p = 0.033, FDR corrected) had significantly decreased f_{IS}, indicating less state transition at HA (Figure 4B). This significant difference only remained in the central region in the theta band (Cz, p = 0.018, FDR corrected). Thus, the brain at HA prefers to dwell in the integration state with less switching frequency, particularly in the left frontal and central parietal regions in all frequency bands.

Network segregation and integration associated with emotional arousal rating

We further investigated whether brain network measures could be used to predict the arousal rating. We collected each global measure from all subjects and then calculated the correlations between pooled measures and pooled arousal rating. This correlation analysis was concentrated on the correspondence between brain activities and emotion rather than individual differences. Insignificant correlations between brain connectivity measures and arousal ratings were observed in all bands on the global scale (all p > 0.05), and we thus turned to the regional study (Figure 5, see Tables S1–S4 for details).

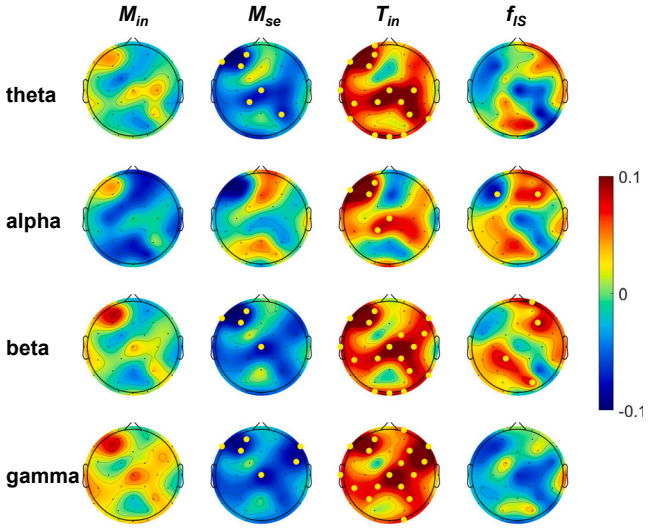

Figure 5. Correlations between brain network measures and arousal ratings

The highlighted electrodes have significant correlations (p < 0.05, FDR corrected).

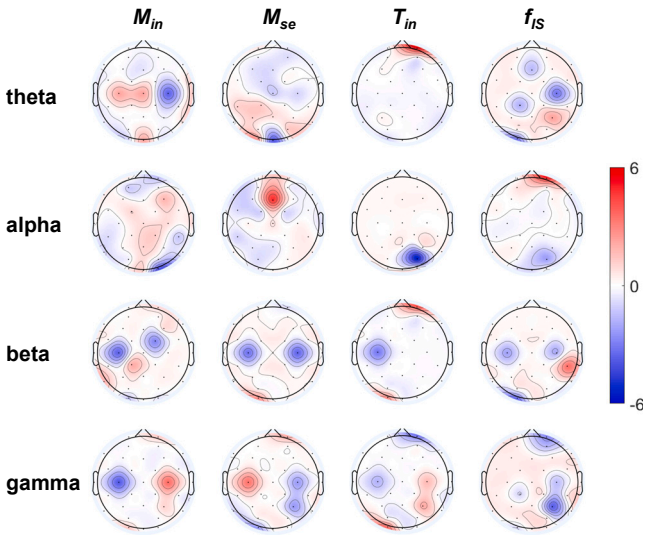

Figure 6. Weights of regions in the prediction models

All of the features were normalized, and the positive/negative weights contributed to higher/lower individual arousal variability.

For the integration strength, none of the regions had a significant correlation with arousal ratings in all bands ($p > 0.05$, FDR corrected). However, the frontal and parietal regions showed negative correlations between M_{se} and arousal ratings in the theta band (AF3, $p = 0.038$; F3, $p = 0.038$; F7, $p = 0.022$; CP1, $p = 0.045$; Cz, $p = 0.045$; P4, $p = 0.045$; FDR corrected), beta band (AF3, $p = 0.006$; F3, $p = 0.006$; F7, $p = 0.006$; Cz, $p = 0.015$; FDR corrected) and gamma band (AF3, $p = 0.032$; F3, $p = 0.023$; F7, $p = 0.032$; Cz, $p = 0.023$; FDR corrected). Significant negative correlations were also observed in the right frontal areas (F8, $p = 0.023$; FC6, $p = 0.023$; FDR corrected) in the gamma band.

Meanwhile, dwell time at integrated state was positively correlated with arousal rating in the frontal and parietal regions (AF3, $p = 0.002$; F3, $p = 0.001$; F7, $p < 0.001$; CP1, $p = 0.020$; FDR corrected). The correlation patterns were similar in the theta, beta, and gamma bands with significantly positive correlations revealed for the frontal, parietal, left temporal and occipital regions.

Finally, the switching frequency results were negatively correlated with arousal ratings in F3 ($p = 0.050$) and positively correlated with that in F4 ($p = 0.050$) in the alpha band. In the beta band, all significant correlations were positive and distributed in the right frontal, parietal, and right occipital regions (F4, $p = 0.011$; CP1, $p = 0.037$; Fp2, $p = 0.008$; PO4, $p = 0.037$; FDR corrected).

In summary, higher emotional arousal is related to weaker network segregation and longer dwell time at the integration state. The significant regions were mainly located in the left frontal, central parietal, and occipital regions, and dwell time was more strongly correlated with emotional arousal.

Individual differences in emotional arousal

Finally, we investigated the association of individual emotional performance with dynamic brain networks. Since the averaged emotional arousal rating has little individual difference (5.157 ± 0.691), we used arousal variability ($V_{arousal,}$ standard deviation/mean of arousal score for each subject) to measure individual performance. Arousal variability showed a high individual difference (0.368 ± 0.127, more details are presented in Figure S2): a higher arousal variability indicates a more sensitive response to emotional stimuli, whereas a lower value reflects a stable emotional arousal condition.

There were no significant correlations between arousal variability and brain network measures at either the global scale or in most regions (more details in Figure S3). Therefore, we adopted a machine learning approach (see STAR Methods) to predict individual arousal variability based on brain network measures. In all frequency bands, M_{in}, M_{se}, $T_{in,}$ and f_{IS} could predict $V_{arousal}$ (all $p < 0.05$), except for M_{se} in the alpha

band (Figure S4), verifying the effectiveness of brain connectivity parameters for predicting individual arousal sensitivity.

We normalized the selected regional features in the prediction models, so regions with positive weights are related to higher $V_{arousal}$, and those with negative weights contribute to lower $V_{arousal}$ Figure 6 . In the prediction model based on integration strength, parietal regions played an important role in predicting individual arousal variability. More specifically, in the theta band, positive weights were found in the left parietal and occipital regions, while negative weights were located in the right parietal regions. In the alpha band, the right occipital, left temporal and prefrontal regions showed negative weights, while the weights were positive but weaker in the broad parietal and right temporal regions. In the beta band, the left parietal (C3), right fronto-central (FC2), and occipital regions (O1, O2) had negative weights. In the gamma band, the weights of the left and right parietal regions were opposite to the results in the theta band, with positive values on the left and negative values on the right.

For segregation strength, the negative weights were distributed in the broad frontal, central, and occipital regions in the theta band. In the alpha band, the highest positive weight was found in the frontal regions, and the right parieto-occipital regions also showed positive values. In higher frequency bands, the parietal regions showed negative weights in the beta band, while in the gamma band, the regions had a negative weight on the left (C3) and positive value on the right (C4). Meanwhile, the right frontal (FP2) and left occipital (O1) regions were also involved in prediction models in the beta and gamma bands.

In the models based on dwell time, the frontal regions showed higher weights in the theta band, while the occipital regions showed negative weights in the alpha band. The right frontal, left occipital, and left parietal regions were involved in the models of the beta and gamma bands.

For switching frequency, the partial regions showed negative weights in theta, beta, and gamma bands, and similar negative weights were found in the left occipital in the theta and beta bands. The positive weights were higher in the left frontal (alpha band) and the right temporal regions (beta band), indicating that more frequent state transitions in such brain regions support higher individual arousal variability. Overall, these results indicate the frequency-specific responsibilities of different regions to individual sensitivity to emotion, especially for the parietal, right prefrontal and left occipital regions.

DISCUSSION

In this study, we applied the NSP method to EEG-based brain functional networks for the first time and investigated the differences in brain functional connectivity patterns under diverse emotional arousal conditions using the NSP analytical approach. First, we found that the brain states were influenced by emotional stimuli, that the integration strength and dwell time were enhanced in the frontal and right posterior parietal regions, and that the segregation strength and flexibility of state transitions were lower in these regions. Second, the comparison of connectivity characteristics between the HA and LA conditions showed significantly decreased segregation strength and increased dwell time of integration in the HA relative to the LA condition in the beta and gamma bands. Moreover, although not significant in all frequency bands, negative correlations were found in M_{se}, whereas T_{in} showed positive correlations with arousal ratings. Finally, connectivity states are reliable for predicting individual differences in emotional arousal. Overall, our results reveal the relationship between dynamic brain states and individual emotional arousal behaviors and further demonstate the effectiveness of the NSP method in measuring EEG-based brain connectivity states.

Frontal and right parietal regions, stable hubs in emotion-related brain networks

To underpin diverse cognitive behaviors, neural information is processed within modules and transferred between modules across large-scale networks.[29,47] The regions called "hubs" participate more in inter-community communications and show stronger integration effects.[48–50] In this study, brain networks showed regional heterogeneous performance during emotional stimuli, with a stronger integration component in the frontal and right posterior parietal regions. The frontal regions, commonly regarded as the emotional regulation system, include the dorsolateral prefrontal, ventrolateral prefrontal, and orbitofrontal cortices and are highly involved in emotion-related behaviors.[51] The increased activation in frontal regions has been shown to be associated with the effective regulation of negative emotion.[11] The parietal regions are involved in several core neurocognitive networks, among them, fronto-parietal networks have

been widely concerned in emotion-related fields because it is fundamental for cognitive functioning, especially in visual tasks.[52–54] Decreased activities in frontal and parietal brain regions are found in depressed patients,[55] and another study on bipolar disorder further showed decreased FC between the frontal-parietal and other brain networks, demonstrating that such emotional disorders are accompanied by a lack of global integration in the frontal and parietal regions. Meanwhile, brain regions including the frontal, temporal, and parietal regions are associated with emotion-related activities.[42,56,57] Our results are consistent with those aforementioned results in that the strength of integration is higher in frontal and parietal regions during emotional video stimuli, further confirming their importance in emotion processing.

In addition to the strength of integration, we also focused on the dynamic reconfiguration of brain networks. Previous studies have identified the modules in brain functional organization based on graph theory and determined the connectivity states by comparing the modularity in FCs.[19,30,58] Such traditional measurements consider the partition of the subsystem as a fixed pattern, which means that the module to which the brain regions belong is unchanged at a given time point.[19,30,58] However, the NSP method allows us to analyze brain connectivity structures at hierarchical levels and consider the comprehensive contributions of integration and segregation at different hierarchical levels. Previous studies have found that NSP measures can reflect the segregation and integration of brain networks, and are more effective in capturing individual differences.[37,59,60] Here, we also compared the results between NSP and graph theory measures (e.g., modularity). Modularity is highly correlated with segregation and integration components from the NSP method (Figure S5), but NSP-based measures can more effectively capture phenotypes of emotional performance (Figure S6). Therefore, NSP is a reasonable and effective method for both EEG- and fMRI-based brain networks. By considering the dwell time, we found that the integration states were predominant in the prefrontal and right posterior parietal regions, particularly the midline in beta and gamma bands. Interestingly, EEG activities of midline regions are associated with emotion processing and have been widely used in emotion recognition.[61] Our results may reveal the neural mechanics of midline (Fz, Cz, Pz) activities influenced by emotional stimuli. We also considered the transition flexibility and higher values reflect more frequent transition between integration and segregation states. Stimulated by emotional videos, the transition flexibility was lower in the hub regions, thus indicating the stable activities of the frontal and right posterior parietal regions in supporting emotional behaviors.

Decreased strength of segregation and increased dwell time of integration under HA condition

tMany studies have investigated the dynamics of brain network organization, demonstrating that the decreased segregation of large-scale brain networks is accompanied by increasing connectivity between brain networks and exhibits dynamic changes in response to cognitive demands.[62] For example, the examination of connectivity states across the healthy adult lifespan has revealed decreasing local segregation with increasing age.[63–65] The age-related difference in segregation may be explained by the changing demands on the brain, such low-modularity organization with lower segregation is found to improve behavior performance during complex tasks, including cognitive control and working memory.[64,66,67] Similarly, decreased segregation has also been found in emotion-related tasks when people respond to threats, which is commonly considered as high arousal condition.[68] Here, we found significantly decreased segregation under HA condition, mainly in the frontal and parietal regions, demonstrating that the brain connected in intensive integrated states with more information communication across distributed regions to maintain high arousal performance. Our results suggest that a high emotional arousal condition is related to increased cognitive load, with brain connectivity becoming more integrated and less segregated.

In addition, the dwell time at the integration state also showed a significant difference between HA and LA conditions. The increased dwell time is associated with HA in most brain regions, demonstrating that the brain dwells longer in at integration state under HA condition, which is consistent with the former explanation that the brain transitions into a state of higher global integration to meet extrinsic task demands.[69]

Since the emotional arousal condition is associated with the degree of activation or deactivation in physiological activity, previous studies have focused on emotion recognition and found that EEG spectral power features as well as network connection parameters are capable of predicting the distinct emotional states of subjects.[4,26] Here, we analyzed the correlation of subjective arousal ratings and the dynamics of brain states and found that the segregation (in theta, beta, and gamma bands) of the frontal and central parietal regions is negatively correlated with arousal ratings, whereas the dwell time at integration state

(in all frequency bands) is positively correlated with arousal ratings involving broader brain regions. The correlations between switching frequency and arousal are positive in the right frontal (in theta and alpha bands), parietal (theta band) regions, and negative in the left frontal regions (alpha band).

Neural activities related to individual emotion arousal

Individual emotion is a highly subjective experience affected by multiple factors, and even the same emotional stimulus can induce different emotional behaviors.[70–72] Dysregulated emotions are usually associated with cognitive performance and mental illness.[73,74] For example, the variability of positive emotion was related to worse psychological health, including depression and anxiety.[75] In addition to the aspect of valence, recent studies have also found that the variability of arousal is positively correlated with cognitive activities such as work vigor.[76] However, little is known about how brain connectivity dynamics change to support individual variability in emotion arousal. Here, we proposed brain connectivity parameters to successfully predict the variability of emotional arousal ratings, further demonstrating the capabilities of dynamic brain states in detecting subjective arousal variability. More importantly, we found that the alpha activity over occipital regions is negatively correlated with the variability of arousal, whereas the theta, beta, and gamma activities are significantly correlated with the variability of arousal in parietal, right prefrontal, and left occipital regions. Thus, these regions play a key role in promoting a more sensitive response between calm and excited states. This finding is partially consistent with a previous finding that alpha activity over the parieto-occipital electrodes is significantly correlated with positive emotional granularity.[70] Our results may offer a way to relate diverse emotional performances to their underlying neurobiological correlates.

Limitations of the study

The EEG signals recorded from scalp electrodes may be a limitation. With only 32 channels, it is not recommended to reconstruct the EEG in the inverse space. Using dense EEG recordings and source estimation method may contribute to further elucidation of the mechanism of emotion. Meanwhile, the current study measured the brain state during emotion stimulus task and lacked a measure of resting recording data. Most studies have revealed that the brain network in the resting state effectively reflects cognitive performance,[77] and additional investigation of resting state could be used as a baseline to lessen individual differences.

STAR★METHODS

Detailed methods are provided in the online version of this paper and include the following:

- KEY RESOURCES TABLE
- RESOURCE AVAILABILITY
  - Lead contact
  - Materials availability
  - Data and code availability
- EXPERIMENTAL MODEL AND SUBJECT DETAILS
- METHOD DETAILS
  - DEAP dataset
  - Brain functional network
  - Nest-Spectral Partition (NSP) method
  - Integration, segregation and balance
  - Dynamic measures of brain connectivity states
  - Regional characteristics of connectivity states
  - Prediction models of individual arousal variability
- QUANTIFICATION AND STATISTICAL ANALYSIS

SUPPLEMENTAL INFORMATION

Supplemental information can be found online at https://doi.org/10.1016/j.isci.2023.106609.

ACKNOWLEDGMENTS

This work was supported by the National Natural Science Foundation of China (Grant No. 12132012, No. 11972275, No. 12272292, No. 11672219), the Natural Science Basic Research Program of Shaanxi (No. 2022JQ-005).

AUTHOR CONTRIBUTIONS

Lv Zhou: conceptuation, methodology, software, formal analysis, writing- original draft, and visualization. Yong Xie: writing-review & editing. Rong Wang: methodology, writing -review & editing. Yongchen Fan: software, writing -review & editing. Ying Wu: conceptuation, writing -review & editing, supervision, funding acquisition.

DECLARATION OF INTERESTS

There are no competing interests pertaining to this article.

Received: October 17, 2022
Revised: February 12, 2023
Accepted: March 31, 2023
Published: April 11, 2023

REFERENCES

1. Anderson, D.J., and Adolphs, R. (2014). A framework for studying emotions across species. Cell *157*, 187–200. https://doi.org/10.1016/j.cell.2014.03.003.

2. Hamann, S., Herman, R.A., Nolan, C.L., and Wallen, K. (2004). Men and women differ in amygdala response to visual sexual stimuli. Nat. Neurosci. *7*, 411–416. https://doi.org/10.1038/nn1208.

3. Veissier, I., and Boissy, A. (2007). Stress and welfare: two complementary concepts that are intrinsically related to the animal's point of view. Physiol. Behav. *92*, 429–433. https://doi.org/10.1016/j.physbeh.2006.11.008.

4. Koelstra, S., Muhl, C., Soleymani, M., Lee, J.-S., Yazdani, A., Ebrahimi, T., Pun, T., Nijholt, A., and Patras, I. (2012). DEAP: a database for emotion analysis ;using physiological signals. IEEE Trans. Affect. Comput. *3*, 18–31. https://doi.org/10.1109/T-AFFC.2011.15.

5. Russell, J.A. (1980). A circumplex model of affect. J. Pers. Soc. Psychol. *39*, 1161–1178. https://doi.org/10.1037/h0077714.

6. McRae, K., Reiman, E.M., Fort, C.L., Chen, K., and Lane, R.D. (2008). Association between trait emotional awareness and dorsal anterior cingulate activity during emotion is arousal-dependent. Neuroimage *41*, 648–655. https://doi.org/10.1016/j.neuroimage.2008.02.030.

7. Talmi, D., Schimmack, U., Paterson, T., and Moscovitch, M. (2007). The role of attention and relatedness in emotionally enhanced memory. Emotion *7*, 89–102. https://doi.org/10.1037/1528-3542.7.1.89.

8. Osugi, A., and Ohira, H. (2017). High emotional arousal enables subliminal detection of concealed information. Psychology *08*, 1482–1500. https://doi.org/10.4236/psych.2017.810098.

9. Schaefer, A., Pottage, C.L., and Rickart, A.J. (2011). Electrophysiological correlates of remembering emotional pictures. Neuroimage *54*, 714–724. https://doi.org/10.1016/j.neuroimage.2010.07.030.

10. Talmi, D., and McGarry, L.M. (2012). Accounting for immediate emotional memory enhancement. J. Mem. Lang. *66*, 93–108. https://doi.org/10.1016/j.jml.2011.07.009.

11. Clark, D.A., and Beck, A.T. (2010). Cognitive theory and therapy of anxiety and depression: convergence with neurobiological findings. Trends Cognit. Sci. *14*, 418–424. https://doi.org/10.1016/j.tics.2010.06.007.

12. Sripada, R.K., King, A.P., Garfinkel, S.N., Wang, X., Sripada, C.S., Welsh, R.C., and Liberzon, I. (2012). Altered resting-state amygdala functional connectivity in men with posttraumatic stress disorder. J. Psychiatry Neurosci. *37*, 241–249. https://doi.org/10.1503/jpn.110069.

13. Davidson, R.J., and Fox, N.A. (1982). Asymmetrical brain activity discriminates between positive and negative affective stimuli in human infants. Science *218*, 1235–1237. https://doi.org/10.1126/science.7146906.

14. Nie, D., Wang, X.-W., Shi, L.-C., and Lu, B.-L. (2011). EEG-based emotion recognition during watching movies. In Proceedings of the 5 International IEEE EMBS Conference on Neural Engineering Cancun, Mexico, p. 670. https://doi.org/10.1109/NER.2011.5910636.

15. Schutter, D.J., Putman, P., Hermans, E., and van Honk, J. (2001). Parietal electroencephalogram beta asymmetry and selective attention to angry facial expressions in healthy human subjects. Neurosci. Lett. *314*, 13–16. https://doi.org/10.1016/S0304-3940(01)02246-7.

16. Zheng, W.-L., Zhu, J.-Y., and Lu, B.-L. (2019). Identifying stable patterns over time for emotion recognition from EEG. IEEE Trans. Affect. Comput. *10*, 417–429. https://doi.org/10.1109/TAFFC.2017.2712143.

17. Wu, X., Zheng, W.-L., Li, Z., and Lu, B.-L. (2022). Investigating EEG-based functional connectivity patterns for multimodal emotion recognition. J. Neural. Eng. *19*, 016012. https://doi.org/10.1088/1741-2552/ac49a7.

18. Anzellotti, S., and Coutanche, M.N. (2018). Beyond functional connectivity: investigating networks of multivariate representations. Trends Cognit. Sci. *22*, 258–269. https://doi.org/10.1016/j.tics.2017.12.002.

19. Fox, M.D., Snyder, A.Z., Vincent, J.L., Corbetta, M., Van Essen, D.C., and Raichle, M.E. (2005). The human brain is intrinsically organized into dynamic, anticorrelated functional networks. Proc. Natl. Acad. Sci. USA *102*, 9673–9678. https://doi.org/10.1073/pnas.0504136102.

20. Mäki-Marttunen, V. (2021). Pupil-based states of brain integration across cognitive states. Neuroscience *471*, 61–71. https://doi.org/10.1016/j.neuroscience.2021.07.016.

21. Sala-Llonch, R., Bartrés-Faz, D., and Junqué, C. (2015). Reorganization of brain networks in aging: a review of functional connectivity studies. Front. Psychol. *6*, 663. https://doi.org/10.3389/fpsyg.2015.00663.

22. Tu, P.-C., Su, T.P., Lin, W.-C., Chang, W.-C., Bai, Y.M., Li, C.-T., and Lin, F.-H. (2019). Reduced synchronized brain activity in schizophrenia during viewing of comedy movies. Sci. Rep. *9*, 12738. https://doi.org/10.1038/s41598-019-48957-w.

23. Zuchowicz, U., Woźniak-Kwaśniewska, A., Szekely, D., Olejarczyk, E., and David, O. (2018). EEG phase synchronization in persons with depression subjected to transcranial magnetic stimulation. Front. Neurosci. *12*, 1037. https://doi.org/10.3389/fnins.2018.01037.

24. Gaviria, J., Rey, G., Bolton, T., Delgado, J., Van De Ville, D., and Vuilleumier, P. (2021). Brain functional connectivity dynamics at rest in the aftermath of affective and cognitive challenges. Hum. Brain Mapp. *42*, 1054–1069. https://doi.org/10.1002/hbm.25277.

25. Nummenmaa, L., Glerean, E., Viinikainen, M., Jääskeläinen, I.P., Hari, R., and Sams, M. (2012). Emotions promote social interaction by synchronizing brain activity across individuals. Proc. Natl. Acad. Sci. USA *109*, 9599–9604. https://doi.org/10.1073/pnas.1206095109.

26. Li, P., Liu, H., Si, Y., Li, C., Li, F., Zhu, X., Huang, X., Zeng, Y., Yao, D., Zhang, Y., and Xu, P. (2019). EEG based emotion recognition by combining functional connectivity network and local activations. IEEE Trans. Biomed. Eng. *66*, 2869–2881. https://doi.org/10.1109/TBME.2019.2897651.

27. Fan, Y., Fan, Q., Zhou, L., Wang, R., Lin, P., and Wu, Y. (2021). Cohesive communities in dynamic brain functional networks. Phys. Rev. E *104*, 014302. https://doi.org/10.1103/PhysRevE.104.014302.

28. Zippo, A.G., Della Rosa, P.A., Castiglioni, I., and Biella, G.E.M. (2018). Alternating dynamics of segregation and integration in human EEG functional networks during working-memory task. Neuroscience *371*, 191–206. https://doi.org/10.1016/j.neuroscience.2017.12.004.

29. Zuberer, A., Kucyi, A., Yamashita, A., Wu, C.M., Walter, M., Valera, E.M., and Esterman, M. (2021). Integration and segregation across large-scale intrinsic brain networks as a marker of sustained attention and task-unrelated thought. Neuroimage *229*, 117610. https://doi.org/10.1016/j.neuroimage.2020.117610.

30. Braun, U., Schäfer, A., Walter, H., Erk, S., Romanczuk-Seiferth, N., Haddad, L., Schweiger, J.I., Grimm, O., Heinz, A., Tost, H., et al. (2015). Dynamic reconfiguration of frontal brain networks during executive cognition in humans. Proc. Natl. Acad. Sci. USA *112*, 11678–11683. https://doi.org/10.1073/pnas.1422487112.

31. Wong, C.H.Y., Liu, J., Lee, T.M.C., Tao, J., Wong, A.W.K., Chau, B.K.H., Chen, L., and Chan, C.C.H. (2021). Fronto-cerebellar connectivity mediating cognitive processing speed. Neuroimage *226*, 117556. https://doi.org/10.1016/j.neuroimage.2020.117556.

32. Shanechi, M.M. (2019). Brain–machine interfaces from motor to mood. Nat. Neurosci. *22*, 1554–1564. https://doi.org/10.1038/s41593-019-0488-y.

33. Madhyastha, T.M., Askren, M.K., Boord, P., and Grabowski, T.J. (2015). Dynamic connectivity at rest predicts attention task performance. Brain Connect. *5*, 45–59. https://doi.org/10.1089/brain.2014.0248.

34. Young, C.B., Raz, G., Everaerd, D., Beckmann, C.F., Tendolkar, I., Hendler, T., Fernández, G., and Hermans, E.J. (2017). Dynamic shifts in large-scale brain network balance as a function of arousal. J. Neurosci. *37*, 281–290. https://doi.org/10.1523/JNEUROSCI.1759-16.2016.

35. Bressler, S.L., and Menon, V. (2010). Large-scale brain networks in cognition: emerging methods and principles. Trends Cognit. Sci. *14*, 277–290. https://doi.org/10.1016/j.tics.2010.04.004.

36. Calhoun, V.D., Miller, R., Pearlson, G., and Adalı, T. (2014). The chronnectome: time-varying connectivity networks as the next frontier in fMRI data discovery. Neuron *84*, 262–274. https://doi.org/10.1016/j.neuron.2014.10.015.

37. Wang, R., Su, X., Chang, Z., Lin, P., and Wu, Y. (2022). Flexible brain transitions between hierarchical network segregation and integration associated with cognitive performance during a multisource interference task. IEEE J. Biomed. Health Inform. *26*, 1835–1846. https://doi.org/10.1109/JBHI.2021.3119940.

38. Li, M., Wu, L., Xu, G., Duan, F., and Zhu, C. (2022). A robust 3D-convolutional neural network-based electroencephalogram decoding model for the intra-individual difference. Int. J. Neural Syst. *32*, 2250034. https://doi.org/10.1142/S0129065722500344.

39. Zhao, Y., Xue, M., Dong, C., He, J., Chu, D., Zhang, G., Xu, F., Ge, X., and Zheng, Y. (2022). Automatic seizure identification from EEG signals based on brain connectivity learning. Int. J. Neural Syst. *32*, 2250050. https://doi.org/10.1142/S0129065722500502.

40. Weng, Y., Liu, X., Hu, H., Huang, H., Zheng, S., Chen, Q., Song, J., Cao, B., Wang, J., Wang, S., and Huang, R. (2020). Open eyes and closed eyes elicit different temporal properties of brain functional networks. Neuroimage *222*, 117230. https://doi.org/10.1016/j.neuroimage.2020.117230.

41. Antonova, I., van Swam, C., Hubl, D., Griskova-Bulanova, I., Dierks, T., and Koenig, T. (2021). Altered visuospatial processing in schizophrenia: an event-related potential microstate analysis comparing patients with and without hallucinations with healthy controls. Neuroscience *479*, 140–156. https://doi.org/10.1016/j.neuroscience.2021.10.014.

42. Yuvaraj, R., Murugappan, M., Acharya, U.R., Adeli, H., Ibrahim, N.M., and Mesquita, E. (2016). Brain functional connectivity patterns for emotional state classification in Parkinson's disease patients without dementia. Behav. Brain Res. *298*, 248–260. https://doi.org/10.1016/j.bbr.2015.10.036.

43. Baczkowski, B.M., Johnstone, T., Walter, H., Erk, S., and Veer, I.M. (2017). Sliding-window analysis tracks fluctuations in amygdala functional connectivity associated with physiological arousal and vigilance during fear conditioning. Neuroimage *153*, 168–178. https://doi.org/10.1016/j.neuroimage.2017.03.022.

44. Li, J., Hua, H., Xu, Z., Shu, L., Xu, X., Kuang, F., and Wu, S. (2022). Cross-subject EEG emotion recognition combined with connectivity features and meta-transfer learning. Comput. Biol. Med. *145*, 105519. https://doi.org/10.1016/j.compbiomed.2022.105519.

45. Wang, R., Lin, P., Liu, M., Wu, Y., Zhou, T., and Zhou, C. (2019). Hierarchical connectome modes and critical state jointly maximize human brain functional diversity. Phys. Rev. Lett. *123*, 038301. https://doi.org/10.1103/PhysRevLett.123.038301.

46. Wang, R., Fan, Y., Wu, Y., Zang, Y.-F., and Zhou, C. (2022). Lifespan associations of resting-state brain functional networks with ADHD symptoms. iScience *25*, 104673. https://doi.org/10.1016/j.isci.2022.104673.

47. Kastrati, G., Thompson, W.H., Schiffler, B., Fransson, P., and Jensen, K.B. (2022). Brain network segregation and integration during painful thermal stimulation. Cerebr. Cortex *32*, 4039–4049. bhab464. https://doi.org/10.1093/cercor/bhab464.

48. Hwang, K., Hallquist, M.N., and Luna, B. (2013). The development of hub architecture in the human functional brain network. Cerebr. Cortex *23*, 2380–2393. https://doi.org/10.1093/cercor/bhs227.

49. Kabbara, A., El Falou, W., Khalil, M., Wendling, F., and Hassan, M. (2017). The dynamic functional core network of the human brain at rest. Sci. Rep. *7*, 2936. https://doi.org/10.1038/s41598-017-03420-6.

50. Sporns, O. (2013). Network attributes for segregation and integration in the human brain. Curr. Opin. Neurobiol. *23*, 162–171. https://doi.org/10.1016/j.conb.2012.11.015.

51. Ertl, M., Hildebrandt, M., Ourina, K., Leicht, G., and Mulert, C. (2013). Emotion regulation by cognitive reappraisal — the role of frontal theta oscillations. Neuroimage *81*, 412–421. https://doi.org/10.1016/j.neuroimage.2013.05.044.

52. Gazzaley, A., Rissman, J., Cooney, J., Rutman, A., Seibert, T., Clapp, W., and D'Esposito, M. (2007). Functional interactions between prefrontal and visual association cortex contribute to top-down modulation of visual processing. Cerebr. Cortex *17 Suppl 1*, i125–i135. https://doi.org/10.1093/cercor/bhm113.

53. Maximo, J.O., Neupane, A., Saxena, N., Joseph, R.M., and Kana, R.K. (2016). Task-dependent changes in frontal–parietal activation and connectivity during visual search. Brain Connect. *6*, 335–344. https://doi.org/10.1089/brain.2015.0343.

54. Zhang, D., and Shen, D.; Alzheimer's Disease Neuroimaging Initiative (2012). Multi-modal multi-task learning for joint prediction of multiple regression and classification variables in Alzheimer's disease. Neuroimage *59*, 895–907. https://doi.org/10.1016/j.neuroimage.2011.09.069.

55. van Heeringen, K., Wu, G.-R., Vervaet, M., Vanderhasselt, M.-A., and Baeken, C. (2017). Decreased resting state metabolic activity in frontopolar and parietal brain regions is associated with suicide plans in depressed individuals. J. Psychiatr. Res. *84*, 243–248. https://doi.org/10.1016/j.jpsychires.2016.10.011.

56. Kouti, M., Ansari-Asl, K., and Namjoo, E. (2022). Emotion discrimination using source connectivity analysis based on dynamic ROI identification. Biomed. Signal Process Control *72*, 103332. https://doi.org/10.1016/j.bspc.2021.103332.

57. Zhang, Y., Yan, G., Chang, W., Huang, W., and Yuan, Y. (2023). EEG-based multi-frequency band functional connectivity analysis and the application of spatio-temporal features in emotion recognition. Biomed. Signal Process Control *79*, 104157. https://doi.org/10.1016/j.bspc.2022.104157.

58. Fukushima, M., Betzel, R.F., He, Y., van den Heuvel, M.P., Zuo, X.-N., and Sporns, O. (2018). Structure–function relationships during segregated and integrated network states of human brain functional connectivity. Brain Struct. Funct. *223*, 1091–1106. https://doi.org/10.1007/s00429-017-1539-3.

59. Chang, Z., Wang, X., Wu, Y., Lin, P., and Wang, R. (2023). Segregation, integration and balance in resting-state brain functional networks associated with bipolar disorder symptoms. Hum. Brain Mapp. *44*, 599–611. https://doi.org/10.1002/hbm.26087.

60. Wang, R., Liu, M., Cheng, X., Wu, Y., Hildebrandt, A., and Zhou, C. (2021). Segregation, integration, and balance of large-scale resting brain networks configure different cognitive abilities. Proc. Natl. Acad. Sci. USA *118*, e2022288118. https://doi.org/10.1073/pnas.2022288118.

61. Zhao, G., Zhang, Y., and Ge, Y. (2018). Frontal EEG asymmetry and middle line power difference in discrete emotions. Front. Behav. Neurosci. *12*, 225.

62. Betzel, R.F., Byrge, L., Esfahlani, F.Z., and Kennedy, D.P. (2020). Temporal fluctuations in the brain's modular architecture during movie-watching. Neuroimage *213*, 116687. https://doi.org/10.1016/j.neuroimage.2020.116687.

63. Chan, M.Y., Park, D.C., Savalia, N.K., Petersen, S.E., and Wig, G.S. (2014). Decreased segregation of brain systems across the healthy adult lifespan. Proc. Natl. Acad. Sci. USA *111*, E4997–E5006. https://doi.org/10.1073/pnas.1415122111.

64. Marek, S., Hwang, K., Foran, W., Hallquist, M.N., and Luna, B. (2015). The contribution of network organization and integration to the development of cognitive control. PLoS Biol. *13*, e1002328. https://doi.org/10.1371/journal.pbio.1002328.

65. Wig, G.S. (2017). Segregated systems of human brain networks. Trends Cognit. Sci. *21*, 981–996. https://doi.org/10.1016/j.tics.2017.09.006.

66. Dai, Z., de Souza, J., Lim, J., Ho, P.M., Chen, Y., Li, J., Thakor, N., Bezerianos, A., and Sun, Y. (2017). EEG cortical connectivity analysis of working memory reveals topological reorganization in theta and alpha bands. Front. Hum. Neurosci. *11*, 237.

67. Yue, Q., Martin, R.C., Fischer-Baum, S., Ramos-Nuñez, A.I., Ye, F., and Deem, M.W. (2017). Brain modularity mediates the relation between task complexity and performance. J. Cognit. Neurosci. *29*, 1532–1546. https://doi.org/10.1162/jocn_a_01142.

68. Kinnison, J., Padmala, S., Choi, J.-M., and Pessoa, L. (2012). Network analysis reveals increased integration during emotional and motivational processing. J. Neurosci. *32*, 8361–8372. https://doi.org/10.1523/JNEUROSCI.0821-12.2012.

69. Shine, J.M., Bissett, P.G., Bell, P.T., Koyejo, O., Balsters, J.H., Gorgolewski, K.J., Moodie, C.A., and Poldrack, R.A. (2016). The dynamics of functional brain networks: integrated network states during cognitive task performance. Neuron *92*, 544–554. https://doi.org/10.1016/j.neuron.2016.09.018.

70. Hu, X., Wang, F., and Zhang, D. (2022). Similar brains blend emotion in similar ways: neural representations of individual difference in emotion profiles. Neuroimage *247*, 118819. https://doi.org/10.1016/j.neuroimage.2021.118819.

71. Phan, K.L., Taylor, S.F., Welsh, R.C., Decker, L.R., Noll, D.C., Nichols, T.E., Britton, J.C., and Liberzon, I. (2003). Activation of the medial prefrontal cortex and extended amygdala by individual ratings of emotional arousal: a fMRI study. Biol. Psychiatr. *53*, 211–215. https://doi.org/10.1016/S0006-3223(02)01485-3.

72. Rui, T., Cui, P., and Zhu, W. (2017). Joint user-interest and social-influence emotion prediction for individuals. Neurocomputing *230*, 66–76. https://doi.org/10.1016/j.neucom.2016.11.054.

73. Fisher, A.C., Rushby, J.A., McDonald, S., Parks, N., and Piguet, O. (2015). Neurophysiological correlates of dysregulated emotional arousal in severe traumatic brain injury. Clin. Neurophysiol. *126*, 314–324. https://doi.org/10.1016/j.clinph.2014.05.033.

74. Rushby, J.A., Fisher, A.C., McDonald, S., Murphy, A., and Finnigan, S. (2013). Autonomic and neural correlates of dysregulated arousal in severe traumatic brain injury. Int. J. Psychophysiol. *89*, 460–465. https://doi.org/10.1016/j.ijpsycho.2013.05.009.

75. Gruber, J., Kogan, A., Quoidbach, J., and Mauss, I.B. (2013). Happiness is best kept stable: positive emotion variability is associated with poorer psychological health. Emotion *13*, 1–6. https://doi.org/10.1037/a0030262.

76. Sosnowska, J., Hofmans, J., and De Fruyt, F. (2019). Relating emotional arousal to work vigour: a dynamic systems perspective. Pers. Indiv. Differ. *136*, 178–183. https://doi.org/10.1016/j.paid.2017.06.040.

77. Betzel, R.F., Cutts, S.A., Greenwell, S., Faskowitz, J., and Sporns, O. (2022). Individualized event structure drives individual differences in whole-brain functional connectivity. Neuroimage *252*, 118993. https://doi.org/10.1016/j.neuroimage.2022.118993.

78. Pedregosa, F., Varoquaux, G., Gramfort, A., Michel, V., Thirion, B., Grisel, O., Blondel, M., Prettenhofer, P., Weiss, R., Dubourg, V., et al. (2011). Scikit-learn: machine learning in Python. J. Mach. Learn. Res. *12*, 2825–2830.

79. Dan, R., Weinstock, M., and Goelman, G. (2022). Emotional states as distinct configurations of functional brain networks. Cerebr. Cortex *2022*, bhac455. https://doi.org/10.1093/cercor/bhac455.

80. Lachaux, J.P., Rodriguez, E., Le Van Quyen, M., Lutz, A., Martinerie, J., and Varela, F.J. (2000). Studying single-trials of phase synchronous activity in the brain. Int. J. Bifurc. Chaos *10*, 2429–2439. https://doi.org/10.1142/S0218127400001560.

81. Lachaux, J.P., Rodriguez, E., Martinerie, J., and Varela, F.J. (1999). Measuring phase synchrony in brain signals. Hum. Brain Mapp. *8*, 194–208. https://doi.org/10.1002/(sici)1097-0193(1999)8:4<194::aid-hbm4>3.0.co;2-c.

82. Lai, M., Demuru, M., Hillebrand, A., and Fraschini, M. (2018). A comparison between scalp- and source-reconstructed EEG networks. Sci. Rep. *8*, 12269. https://doi.org/10.1038/s41598-018-30869-w.

83. Aydore, S., Pantazis, D., and Leahy, R.M. (2013). A note on the phase locking value and its properties. Neuroimage *74*, 231–244. https://doi.org/10.1016/j.neuroimage.2013.02.008.

84. Sarmukadam, K., Bitsika, V., Sharpley, C.F., McMillan, M.M.E., and Agnew, L.L. (2020). Comparing different EEG connectivity methods in young males with ASD. Behav. Brain Res. *383*, 112482. https://doi.org/10.1016/j.bbr.2020.112482.

85. Santamaria, L., Noreika, V., Georgieva, S., Clackson, K., Wass, S., and Leong, V. (2020). Emotional valence modulates the topology of the parent-infant inter-brain network. Neuroimage *207*, 116341. https://doi.org/10.1016/j.neuroimage.2019.116341.

86. Kabbara, A., Paban, V., and Hassan, M. (2021). The dynamic modular fingerprints of the human brain at rest. Neuroimage *227*, 117674. https://doi.org/10.1016/j.neuroimage.2020.117674.

87. Belkin, M., and Niyogi, P. (2001). Laplacian eigenmaps and spectral techniques for embedding and clustering. Adv. Neural Inf. Process. Syst. *14*, 585–591.

88. Jin, F., Xiao, F.W., and Xiang, L. (2007). Enhancing synchronizabilities of power-law networks. In IEEE International Symposium on Circuits & Systems. https://doi.org/10.1109/iscas.2007.377956.

STAR★METHODS

KEY RESOURCES TABLE

REAGENT or RESOURCE	SOURCE	IDENTIFIER
Biological samples		
EEG data	DEAP project	http://www.eecs.qmul.ac.uk/mmv/datasets/deap/
Software and algorithms		
MATLAB R2019b	MathWorks	https://github.com/pibubu/emotion-NSP
scikit-learn toolbox	Pedregosa et al.[78]	https://scikit-learn.org/stable/index.html
pwr R package	CRAN	https://cran.r-project.org/web/packages/pwr/

RESOURCE AVAILABILITY

Lead contact

Further information and requests for resources and reagents should be directed to and will be fulfilled by the lead contact, Ying Wu (wying36@mail.xjtu.edu.cn).

Materials availability

This study did not generate new unique reagents.

Data and code availability

- The EEG data were acquired from DEAP project with the permission authorized from http://www.eecs.qmul.ac.uk/mmv/datasets/deap/.
- All original code has been deposited at https://github.com/pibubu/emotion-NSP.
- Any additional information required to reanalyze the data reported in this paper is available from the lead contact upon request.

EXPERIMENTAL MODEL AND SUBJECT DETAILS

The DEAP dataset contains the EEG signals of 32 healthy participants (16 females, age:27.19±4.38) when they watched 40 one-minute long excerpts of music videos.[4] Post-hoc power analysis (Cohen's effect = 0.6, sample size = 32, significance level = 0.05, type = paired) showed a power of 0.91. The 40 trials were chosen among 120 music videos and were shown to effectively induce an emotional response. The EEG signals were recorded with 32 channels according to the international 10-20 system, involving a sampling rate of 512 Hz. Each trial had a 63 s EEG recording. The first 3 s was recorded in the resting state and was deleted here. The remaining 60 s was recorded during video clips. Thus, the EEG data dimension for each participant was 40 trials × 32 channels × 60 s.

METHOD DETAILS

DEAP dataset

The self-assessments of participants include continuous levels of arousal, valence, like/dislike, dominance, and familiarity. The valence-arousal dimension can be divided into four categories: high-arousal high-valence, low-arousal high-valence, low-arousal low-valence and high-arousal low-valence.[4] However, the mapping between emotional states and modular brain representations can be many-to-one,[79] resulting in great challenges to conclude whether the altered dynamic brain states are specific to arousal or valence. Therefore, according to previous studies,[7,8,10] we focused only on the arousal dimension. Arousal was rated from 1∼9 directly after watching each video, and a higher score indicated a more excited emotional condition.[5] To avoid ambiguity in moderately rated areas, we set low arousal (LA) condition trials with ratings of 1∼4 and high arousal (HA) condition trials with ratings of 6∼9. Thus, the 40 trials for each participant were divided into 2 types: LA or HA.

In the DEAP dataset, EEG signals were preprocessed using EEGLAB with following the five steps: 1) down-sampling to 128 Hz, 2) removal of eye artifacts with a blind source separation technique by independent component analysis (ICA) using the AAR plugin, 3) bandpass filtering from 4.0-45 Hz, 4) averaging to common reference, and 5) segmenting into 60 s with the 3 s pre-trial baseline removed.[4]

Brain functional network

The Finite Impulse Response (FIR) bandpass filter was used to further filter EEG signals to different frequency bands (θ:4-7; α:8–13 Hz, β:14–30 Hz, and γ: 30–45 Hz). In each band, dynamic functional connectivity (dFC) was constructed by calculating the phase locking value (PLV)[80,81] between any two EEG channels. Even PLV may suffer from signal leakage and volume conduction,[82] and it has advantages in calculating the non-stationary and non-linear interactions between neural signals[83,84] by separating the phase and amplitude of signals and thus has been widely used in emotion-related functional network analysis.[26,57,85] Meanwhile, PLV directly measures the instantaneous phase synchrony separately from the amplitude component in a given frequency band and determines the length of sliding windows. The PLV is defined as:

$$PLV(t) = \left| \frac{1}{\delta} \int_{t-\delta/2}^{t+\delta/2} e^{j\left(\varphi_y(\tau) - \varphi_x(\tau)\right)} d\tau \right| \quad \text{(Equation 1)}$$

Here, $\varphi_x(\tau)$ and $\varphi_y(\tau)$ are the instantaneous unwrapped phases of signals x and y in the given frequency at time point t, which were extracted through the Hilbert transform. δ denotes the width of the sliding time window and should satisfy $n_{cy} = f_{central} \cdot \delta$. As recommended by Lachaux, $n_{cy} = 6 \sim 10$[80], here we used $n_{cy} = 6$[49,86], and the corresponding δ values were 1.2 s, 0.57 s, 0.27 s, 0.16 s in theta, alpha, beta and gamma bands, respectively. The results were similar for $n_{cy} = 8$ and 10 (see Figures S7–S9). PLV ranges from 0 to 1, and a higher value indicates a stronger degree of synchronization between the calculated pairs, and a lower value reflects weaker connectivity. Since there were only 32 channels, we calculated the PLV between all 32 pairs of channels for each time window in a specific band and ultimately obtained a series of time-resolving 32×32 weighted, undirected matrices C_t.

Nest-Spectral Partition (NSP) method

The NSP method is effective in quantifying functional segregation and integration across multiple levels.[46] Based on the eigenmodes, the brain regions can be partitioned into multiple modules at different levels. Each brain functional matrix C_t is symmetric and could be decomposed into $C_t = W\Sigma W^T$, where each column of W is the eigenvector corresponding to the eigenvalue in Σ. After arranging the eigenvalues in descending order, we obtained a new eigenvalue matrix Λ and eigenvector matrix U. NSP detects modules in different levels based on eigenvectors. In the 1st mode, all channels had the same negative or positive eigenvector value, and this mode was regarded as the first level, with one module (i.e., whole-brain network). In the 2nd mode, the channels with positive eigenvector signs were assigned to a module, and the regions with negative signs formed the second module. This mode was regarded as the second level, with two modules. Based on the positive or negative sign of channels in the 3rd mode, each module in the second level was further partitioned into two submodules, forming the third level. Subsequently, the FC network could be modularly partitioned into multiple levels with the order of functional modes increasing (see Figure 1). Channels within a module in a level may have the same sign of eigenvector values in the next level, and then the module is indivisible, which has no effect on the subsequent partitioning process. When each module contained only a single channel at a given level, the partitioning process was stopped. After the partitioning process, the NSP method outputs, the module number M and module size m. We then calculated the weighted module number H in the ith level:

$$H_i = \Lambda_i^2 M_i (1 - p_i) / N \quad \text{(Equation 2)}$$

where Λ_i is the eigenvalue of functional modes; M_i is the module number in the ith level; N is the number of rows/columns of the matrix; $p_i = \sum \left| m_{ij} - 1/M_i \right| / N$ is a corrected factor that reflects the deviation from the evenly distributed modular size at this level; and m_{ij} is the modular size in the jth module at the ith level. Apparently, the NPS method combines the information eigenvalues and eigenvectors of brain functional networks, which is different from the previous spectral analyses, e.g., eigenvalue-based power-law analysis and eigenvector-based spectral embedding/clustering,[87,88] and has clearer physic meaning for segregation and integration.

Integration, segregation and balance

The divided modules could be regarded as functional brain regions at the specific hierarchical level. Communications within modules correspond to local segregation and information processing across other modules indicates global integration. At the 1st level, all elements of eigenvectors are positive, indicating global attributes of intrabrain communication. We calculated H_{in} to assess the effective global integration.

$$H_{in} = H_1 / N = \Lambda_1^2 M_1 (1 - p_1) / N^2 \quad \text{(Equation 3)}$$

Higher levels included more than one module to support functional segregation.

We calculated brain segregation by averaging the H_i from the 2nd to the Nth levels to evaluate the total degree of local segregation in each hierarchical functional organization, where information processes are strong within modules.

$$H_{se} = \sum_{i=2}^{N} H_i / N = \sum_{i=2}^{N} \Lambda_i^2 M_i (1 - p_i) / N^2 \quad \text{(Equation 4)}$$

The deviation from the balance state, where segregation equals integration, was defined as:

$$H_B = H_{in} - H_{se} \quad \text{(Equation 5)}$$

The results of H_{in}, H_{se} and H_B dynamically changed during the entire recording period and the temporal fluctuations of the hierarchical community indicated that the human brain dynamically reorganizes to satisfy complex mental demands, and the degree of brain states also varies over time (Figure 1E).

Dynamic measures of brain connectivity states

Based on the hierarchical module method, each node participates in different modules to support complex neural information processing, integrated in some levels and segregated in others. Both integration and segregation have been proven to be associated with cognitive performance, and integration is particularly highly related to arousal fluctuations. We defined M_{in} and M_{se} to evaluate brain integration and segregation separately.

$$M_{in} = \sum_{t=1}^{N} H_{in}(t)/N \quad \text{(Equation 6)}$$

$$M_{se} = \sum_{t=1}^{N} H_{se}(t)/N \quad \text{(Equation 7)}$$

In addition, we further analyzed the dynamics of brain state transitions. The dwell time of integration T_{in} and switching frequency f_{IS} were measured to characterize the dynamic balance state, where $|H_{in}| = |H_{se}|$.

$$T_{in} = t_{H_B(t) \geq 0 / t_{all}} \quad \text{(Equation 8)}$$

Here, T_{in} measures the percentage of the integrated state ($H_B \geq 0$) across all the time windows. A higher T_{in} indicates that the integrated function is dominant during the entire recording.

$$f_{IS} = n_{H_B(t) \cdot H_B(t+1) \leq 0 / t_{all}} \quad \text{(Equation 9)}$$

f_{IS} represents the frequency of brain network switching between the two connectivity states. Increased f_{IS} indicates a more flexible connectivity transition between integration and segregation.

Regional characteristics of connectivity states

Furthermore, we calculated the regional weighted module number $H_{i,channel}$ for each channel,

$$H_{i,channel} = H_i \cdot u_{i,channel}^2 = \frac{\Lambda_i^2 M_i (1 - p_i)}{N} \cdot u_{i,channel}^2 \quad \text{(Equation 10)}$$

where $u_{i,channel}$ is the eigenvector value of the analyzed channel in the ith hierarchical level.

Then, we could measure the nodal integration, segregation, balance ($H_{in,channel} = \frac{H_{1,channel}}{N}$, $H_{se,channel} = \sum_{i=2}^{N} \frac{H_{i,channel}}{N}$, $H_{B,channel} = H_{in,channel} - H_{se,channel}$) and the related dynamic characteristics ($M_{in,channel}$, $M_{se,channel}$, $T_{in,channel}$, $f_{IS,channel}$) for each channel.

Prediction models of individual arousal variability

To predict individual arousal variability, we constructed multiple linear regression (MLR) models using the *scikit-learn* toolbox. Taking regional connectivity state parameters (M_{in}, M_{se}, T_{in}, *and* f_{IS}) as independent variables (x) and $V_{arousal}$ as the dependent variables (y), we first calculated the correlations between $V_{arousal}$ and the regional features and then reordered the regional parameters according to the calculated F-statistic. Second, we selected the first K regions and fed the corresponding features into the MLR. Third, the leave-one-out cross-validation (LOO-CV) method was applied to validate the prediction model. The predicted $V_{arousal}$ based on the subset of regional parameters was evaluated by the correlations between real and predicted scores, after which the best prediction model with k features was identified. Furthermore, we compared the weights of selected regional parameters after normalizing the features to determine how important those regions are in supporting the individual emotion experiences.

QUANTIFICATION AND STATISTICAL ANALYSIS

Statistical analyses of high and low arousal conditions were performed in MATLAB using two-sample t-test. Pearson correlation coefficient were used to calculated the correlations between brain network measures and arousal ratings. The significance cutoff for all comparisons was $p<0.05$. The the *scikit-learn* toolbox was used to construct the MLR models. Post-hoc power analysis were performed to validate the effectiveness of dataset using *pwr* package in *R* v4.1.2.